Advances in Materials Science for Environmental and Energy Technologies VI

Edited by
Tatsuki Ohji
Josef Matyáš
Henry Colorado
Raghunath Kanakala

Ceramic Transactions
Volume 262

The American Ceramic Society

WILEY

Advances in Materials Science for Environmental and Energy Technologies VI

Advances in Materials Science for Environmental and Energy Technologies VI

Ceramic Transactions, Volume 262

Edited by

Tatsuki Ohji
Josef Matyáš
Henry Colorado
Raghunath Kanakala

WILEY

This edition first published 2017
© 2017 The American Ceramic Society

All rights reserved. No part of this publication may be reproduced, stored in a retrieval system, or transmitted, in any form or by any means, electronic, mechanical, photocopying, recording or otherwise, except as permitted by law. Advice on how to obtain permission to reuse material from this title is available at http://www.wiley.com/go/permissions.

The rights of Tatsuki Ohji, Josef Matyáš, Henry Colorado, and Raghunath Kanakala to be identified as the authors of the editorial material in this work have been asserted in accordance with law.

Registered Office
John Wiley & Sons, Inc., 111 River Street, Hoboken, NJ 07030, USA

Editorial Office
111 River Street, Hoboken, NJ 07030, USA

For details of our global editorial offices, customer services, and more information about Wiley products visit us at www.wiley.com.

Wiley also publishes its books in a variety of electronic formats and by print-on-demand. Some content that appears in standard print versions of this book may not be available in other formats.

Limit of Liability/Disclaimer of Warranty
In view of ongoing research, equipment modifications, changes in governmental regulations, and the constant flow of information relating to the use of experimental reagents, equipment, and devices, the reader is urged to review and evaluate the information provided in the package insert or instructions for each chemical, piece of equipment, reagent, or device for, among other things, any changes in the instructions or indication of usage and for added warnings and precautions. While the publisher and authors have used their best efforts in preparing this work, they make no representations or warranties with respect to the accuracy or completeness of the contents of this work and specifically disclaim all warranties, including without limitation any implied warranties of merchantability or fitness for a particular purpose. No warranty may be created or extended by sales representatives, written sales materials or promotional statements for this work. The fact that an organization, website, or product is referred to in this work as a citation and/or potential source of further information does not mean that the publisher and authors endorse the information or services the organization, website, or product may provide or recommendations it may make. This work is sold with the understanding that the publisher is not engaged in rendering professional services. The advice and strategies contained herein may not be suitable for your situation. You should consult with a specialist where appropriate. Further, readers should be aware that websites listed in this work may have changed or disappeared between when this work was written and when it is read. Neither the publisher nor authors shall be liable for any loss of profit or any other commercial damages, including but not limited to special, incidental, consequential, or other damages.

Library of Congress Cataloging-in-Publication Data is available
ISBN: 9781119423768
ISSN: 1042-1122

Cover design by Wiley

10 9 8 7 6 5 4 3 2 1

Contents

CONSTRUCTION AND BUILDING MATERIALS FOR A BETTER ENVIRONMENT

MATERIALS ISSUES IN NUCLEAR WASTE MANAGEMENT IN THE 21ST CENTURY

Preface

This volume contains 20 papers presented during the Materials Science & Technology 2016 Conference (MS&T'16), held October 23–27, 2016 at the Salt Palace Convention Center, Salt Lake City, Utah. Papers from the following symposia are included in this volume:

- 8th International Symposium on Green and Sustainable Technologies for Materials Manufacturing and Processing
- Construction and Building Materials for a Better Environment
- Materials Issues in Nuclear Waste Management in the 21st Century
- Materials Development for Nuclear Applications and Extreme Environments
- Nanotechnology for Energy, Healthcare, and Industry
- Materials and Processes for CO_2 Capture, Conversion, and Sequestration

The success of these symposia and the publication of the proceedings could not have been possible without the support of The American Ceramic Society and other organizers of the program. The program organizers and session chairs for the above symposia are appreciated. Their assistance, along with that of the reviewers was invaluable in ensuring the creation of this volume.

Tatsuki Ohji, AIST, JAPAN
Josef Matyáš, Pacific Northwest National Laboratory, USA
Henry Colorado, Universidad de Antioquia, Colombia
Raghunath Kanakala, University of Idaho, USA

Green and Sustainable Technologies for Materials Manufacturing and Processing

TITANIA NANOSHEET PRODUCTION BY AN INEXPENSIVE GREEN PROCESS

Cody Cannon and Allen W. Apblett
Oklahoma State University
Stillwater, OK, USA

ABSTRACT

Anatase nanosheets were synthesized via a facile green process that involved isothermal aging of a titanyl sulfate solution at 60 °C. The process produced two distinct titanium products a stable colloid composed of anatase nanosheets that were on average 1.53 nm or approximately 4 unit cells in height. Due to a preferential growth axis the nanosheets imaged by TEM displayed the (101) face of anatase. The colloids had a markedly high band gap of 3.82 eV, which is higher than typical for nanoparticles of similar dimensions and was only reported in one other synthesis for nanosheets. This increase in the band gap can be contributed to the 2D quantum confinement of the nanosheets. The precipitated solid was also characterized and determined to be anatase nanosheets. The nanosheets in the precipitates were found to be on average 3.93 nm in thickness. This equates to roughly 11 unit cells on average. The precipitates tended to form aggregates that were on average 96.9 nm in diameter as measured by AFM. The sheets in both cases were found to have a preferential growth axis and the lattice fringes of the (101) anatase planes were very evident in the TEM images of both materials. The aggregated anatase nanosheets were found to be photocatalytic and were able to oxidize methylene blue. Titanium nanosheets with (101) exposed faces are of particular interest for many applications including dielectrics, photovoltaics, and photocatalysis due to the many exposed defects on the surface giving rise to unique properties.

INTRODUCTION

The discovery of the photocatalytic splitting of water by Fujishima and Honda using titanium dioxide and ultraviolet light has encouraged a large amount of research in TiO_2 [1]. Titanium (IV) oxide has been shown to be extremely versatile and has many applications in areas such as photocatalysis[1], UV filters,[2-3] water purification [4-5] and solar cells [6-8] to name a few. In the past few years a new push in titanium research has focused on methods for the preparation and applications of nanosized titanium particles [9-11]. These nanoparticles are of great interest due to their potential to have unique properties in comparison to the bulk materials that will meet the needs for a wide variety of applications.

The increase in surface area of nanomaterials as the surface to volume ratio increases with decreasing particle size often results in increased reactivity due to an increase in surface active sites. Anatase nanoparticles are of particular interest because their photocatalytic properties are superior to the other two phases of TiO_2, brookite and rutle [12]. echniques including sol-gel [13-14], hydrothermal methods [15], and gas condensation [16]. The hydrothermal method utilizes titanium salts that undergo hydrolysis under specific conditions to form titanium dioxide and is one of the most robust and tunable methods. There are many methods used for the hydrothermal production of photoactive titanium oxide. Bavykin et al. used a seeded titanium sulfate solution with reflux and various acid types to investigate the impact on morphology [17]. The author observed that hydrolysis occurred slowly at 70°C under reflux conditions and that anatase phase particles only formed after prolonged reflux. It was also shown that a wide variety of titanium materials with different particle sizes can be tailor made by just fine tuning the acid concentrations or by the addition of a second mineral acid. Seishiro et al. were able to produce anatase phase titanium using ethanol and titanium sulfate under reflux via hydrolysis resulting in the synthesis of anatase TiO_2 [18]. There are many other hydrothermal synthesis that produce

photoactive anatase titanium but all involve refluxing or the use of an organic templating agent or seed nuclei, or high temperature calcining in order to produce the anatase phase product.

In this investigation a low temperature isothermal method was applied to an aqueous titanium sulfate solution in order to produce two separate nanometric titanium products. The first of these is a nanocrystalline anatase titanium dioxide aggregate that has photocatalytic properties. This synthesis also results in the preparation of a stable aqueous titanium dioxide colloidal suspension. This colloid consists of anatase phase nanosheets that are stable for more than six months of storage.

EXPERIMENTAL

Materials and Methods

The titanium sulfate used was obtained from Alfa-Aesar and all other chemical reagents used in the experiments were all obtained from commercial sources with ACS-grade purities and were used without further purification. Water was purified by reverse osmosis followed by deionization. X-ray powder diffraction (XRD) was performed using a Bruker D8 powder diffractometer in order to analyze the structural properties of the synthesized titanium powder. Morphological features of the powder samples and colloid were determined using transmission electron microscopy (JOEL JEM-2100). The solid sample was embedded and sectioned in order to image the sample by transmission electron microscopy while a drop of the colloid solution was allowed to evaporate on a TEM grid and then imaged. BET nitrogen adsorption measurements were made using a Quantacrome Nova 1200 to determine the surface area of the synthesized titanium dioxide nanoparticles. Atomic force microscopy was used in tapping mode to determine the height of the colloid particles and the precipitate. Both samples were placed on a clean piece of mica by placing a drop on the surface and allowing it to evaporate. The precipitate was suspended and allowed to settle prior to placing the drop on the mica. Raman and IR spectra were collected for the synthesized nanoparticles using a Nicolet NXR 9610 FT-Raman spectrometer with a fixed laser of 976 nm and a Nicolet 750 FT-IR instrument. The FT-IR spectra were collected by grinding the precipitated samples with KBr and pressing the sample into a transparent pellet that was then run in transmittance mode on the FT-IR. Particle size analysis of the colloid and an aqueous suspension of the prepared nanoparticles was performed using a Malvern HPP5001 dynamic light scattering instrument. UV-Visible spectra of the suspended nanoparticles and the colloid were recorded using a Cary 100 UV- Visible spectrometer.

Synthesis of Titania Nanosheets

A titanyl sulfate solution (0.2 M) was prepared in an Erlenmeyer flask by adding 12.01 g (.083 moles) of titanium oxide sulfate sulfuric acid hydrate to 200 mL of deionized water. A half of a molar equivalent of concentrated sulfuric acid (4.28 g) was then added (4.18 g) and the solution was carefully heated with stirring. As the titanyl sulfate dissolved the white color faded and the solution turned transparent. As soon as this occurred, the flask was removed from the heat and allowed to cool to room temperature. It was then placed in a screw cap glass bottle and heated at 60 °C for 72 hours. During this time, a white precipitate formed that was isolated by centrifugation at 3000 RPM for 1 hour. The supernatant was a colloidal suspension that was poured off and saved. The solid was then washed three additional times with 200 mL aliquots of deionized water by a resuspending/centrifugation process. The suspension was stored in a glass bottle while the solid was vacuum dried at 1 atm until a constant weight was achieved. After drying 1.72 g of the titanium precipitate product was obtained corresponding to a 26 percent yield based on the hypothesis that all of the available titanium in the solution was precipitated as titanium dioxide. Assuming that the remaining titanium is in solution as the colloid,

approximately 74 percent (4.9g) of the titanium dioxide is present in the colloid. This would give the colloid a concentration of 0.31 M. The titanium content determined gravimetrically was 85% corresponding to 1.46g of titanium dioxide.

RESULTS AND DISCUSSION

X-ray powder diffraction demonstrated that the titanium dioxide precipitate that was formed was composed exclusively of nanocrystalline anatase phase of titanium dioxide. This is illustrated by the excellent match to the ICCD powder diffraction file (# 03-065-5714) and the absence of any characteristic peaks of rutile or brookite phases at 27° and 31° respectively in the pattern (Figure 1). The broadening of the XRD peaks is characteristic of a nanocrystalline material, indicating that the material is an aggregate of nanocrystalline anatase titanium that has some long-range order since XRD gives an average of the order over several unit cells. The Scherrer equation. used to calculate the crystallite size of the titanium aggregates using the (101) peak, indicated that the lower boundary on the particle size was 11.2 nm.

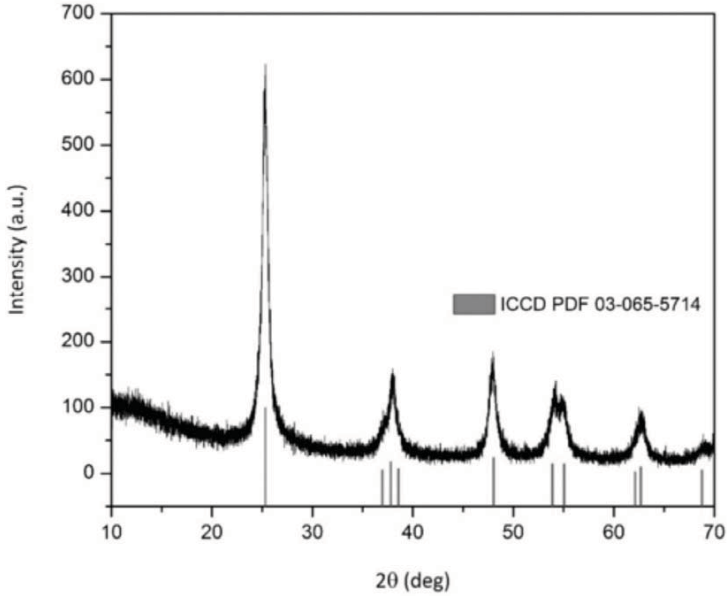

Figure 1. X-Ray Powder Diffraction Pattern of Titanium Nanosheet Precipitate with the ICDD Diffraction Pattern File for Anatase in Grey.

Transmission electron microscopy was used to determine the morphology of the materials. The colloid material was diluted 1000 fold and then drop cast onto a copper TEM grid and allowed to air dry. The TEM micrographs showed that the particles aggregated during the drying process (Figure 2A). The nanoparticles have no discernable uniform shape but they do appear to have very flat surfaces and they also have very low contrast with the grid. These facts suggest that the colloid is composed of nanosheets of titanium dioxide. The particles range in size from 4.0 nm to 7.0 nm in diameter. The lattice fringes of the titanium colloid are visible in Figure 2B. When the particles are measured from fringe edge to fringe edge they are also found

to range in size from 4.0 to 7.0 nm. The lattice fringes occupy the entire volume of the particles indicating they are single crystals. Image J software was used to measure the spacing between lattice fringes of a number of particles in the image. These were all found to have the same spacing of 3.5 Å that corresponds to the (101) face of anatase. This face is a step edge that is composed of monoatomic height steps and is the most commonly observed crystal face in anatase titanium dioxide[19]. The (101) surface is of great interest because of the potential photocatalytic and solar cell applications of TiO_2[20-21].

The precipitated titanium dioxide was prepared for electron microscopy by suspending the particles in deionized water and sonicating for one hour. The suspension was then drop cast onto a copper TEM grid and the water was allowed to evaporate (Figure 2C). These particles are much larger in size than the colloid particles and are also aggregated. The crystallites were flat and the lattice fringes could easily be observed and made up the entire volume of the observed particles. Like the colloid the particles appeared to be flat and gave low contrast indicating that the aggregates were composed of thin nanosheets. The suspended particles had a crystallite size ranging from 10 nm to 35 nm and formed aggregates that are between 100 to 300 nm in diameter. The spacing of the lattice fringes was 3.5 Å corresponding to the 101 planes of anatase.

In order to determine if the aggregation seen in the micrographs was due to the technique used in preparing the samples for TEM or if it was occurring in solution the precipitated sample was also embedded in resin, (Figure 2D) sectioned with a microtome, and then imaged. TEM micrographs of the sections material showed aggregated crystallites that matched those observed in the suspended samples in both size and morphology. This confirms that aggregation occurred during the precipitation process and was not an artifact of TEM sample preparation.

The results from the TEM and XRD characterization indicate that during the static 60°C heating process the formation of anatase phase titanium nanosheets takes place. Through centrifugation it was possible to separate the aggregates from the suspended nanosheets of titanium dioxide resulting in isolation of both a stable colloidal suspension of anatase nanosheets and a nanocrystalline aggregate of anatase nanosheets. The phase of both the products was confirmed through d spacing measurements in the TEM and the powder X-ray diffraction pattern of the precipitated solid. The phase identification for the colloid is based on the d spacing measurements of the TEM only.

From the TEM and XRD results a hypothesis can be made concerning the process of the formation of the particles. When the solution is isothermally heated at 60°C the nucleation of nanometric titanium dioxide particles begins slowly over time resulting in the formation of anatase nanosheets. Once these particles grow and reach about 10 nm in diameter they began to aggregate and form nanocrystalline solids that precipitate out of solution. This is supported by both the TEM and XRD results since all of the observed particles in the colloid by TEM were measured to be less than 10 nm in diameter. From the XRD we can use the Scherrer equation to determine the lower limit of the crystallite size of the sample by measuring the full width of the peak at half height. The titanium precipitate gave a lower boundary of 11.2 nm, further supporting the idea that the sheets are aggregating once they reach about 11 nm in diameter. If this were not the case we would have expected a much smaller value for the Scherrer calculation since particles of a smaller diameter were readily available in solution to be incorporated into the precipitates. From the TEM results, it can be estimated that the aggregates have crystallite size ranging from 10 to 35 nm. This indicates that the particles still grow once they have fallen out of solution and aggregated leading to many crystallites larger than 10 nm in diameter in the precipitated nanosheet aggregates.

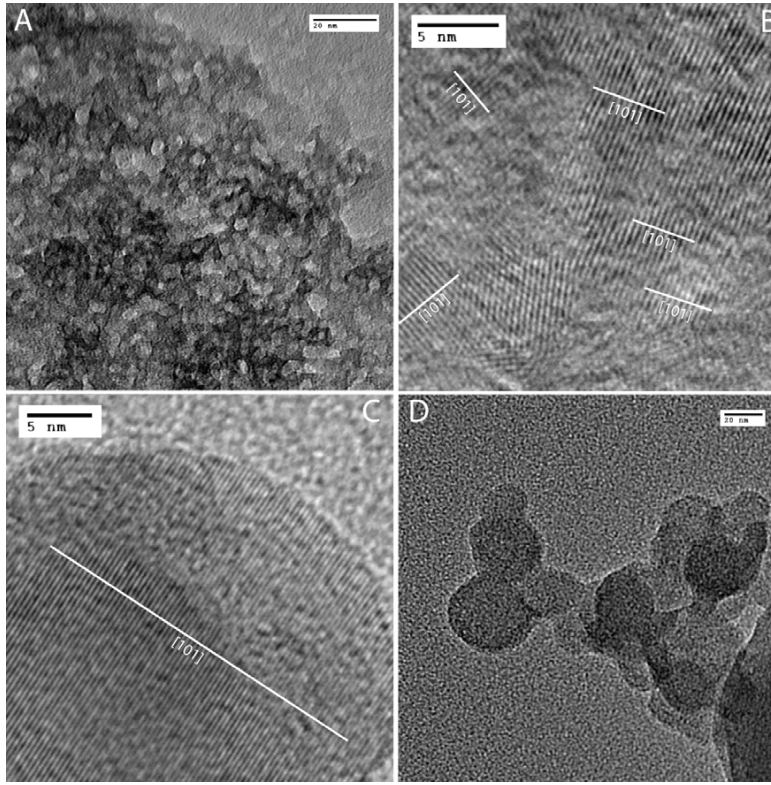

Figure 2. TEM images of (A) titanium colloid nanosheets, (B) titanium colloid nanosheets with visible lattice fringes, (C) precipitated titanium nanosheets with visible lattice fringes, and (D) precipitated titanium nanosheets embedded and sectioned

Atomic force microscopy (AFM) was used in order to confirm that the findings of the TEM images that the particles were nanosheets. The AFM images were obtained in tapping mode and the height, width, and length of the particles were determined. The colloid sample aggregated when being placed on the mica causing the diameter measurements to not be usable but the height of the nanosheets could still be determined. The software was set to measure the height from the mica to the surface of the titanium nanosheets. Figure 3 shows the height of the nanosheets from the colloid samples based on the height measurements. The mean height of the colloid sample from 82 measurements was found to be 1.53 nm with a maximum of 3.22 nm and a minimum of 0.37 nm. The AFM image of the precipitated particles is shown in Figure 4. From this data it was possible to measure both the heights and diameters of the precipitated particles. The height based on 52 measurements was found to have a mean of 3.93 nm with a minimum of 1.28 nm and a maximum of 5.74 nm. The diameter was also based on 52 measurements and was found to be 96 nm with a minimum of 55 nm and a maximum of 182 nm.

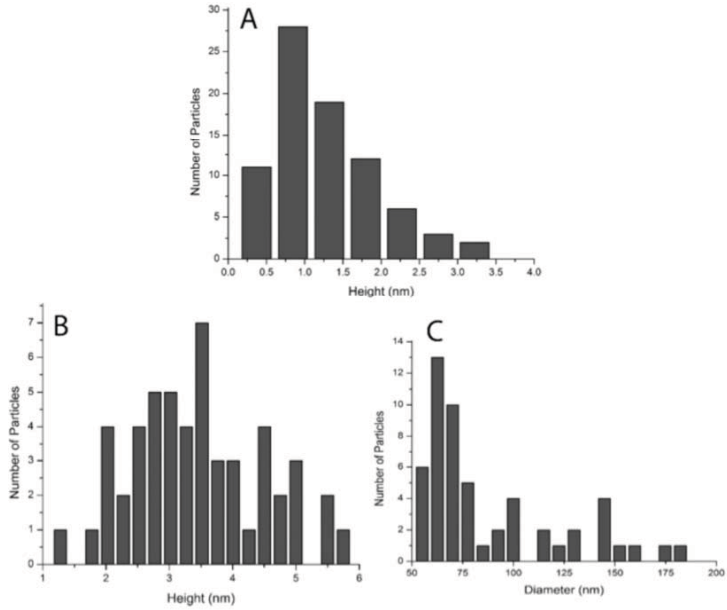

Figure 3 (A) Distribution of Height Measurements of (A) Titanium Colloid Nanosheets (B) Precipitated Titanium Nanosheets (C) Distribution of Diameter Measurements of Precipitated Titanium Nanosheets

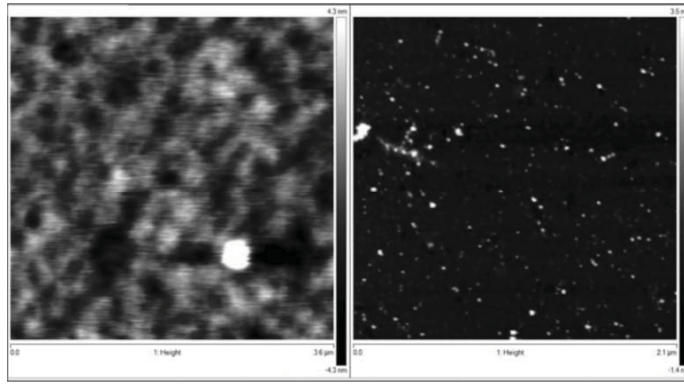

Figure 4. Atomic Force Microscopy Images of Titanium Colloid Nanosheets (Left) and Precipitated Titanium Nanosheets (Right)

Since the particle size measurements from both the AFM and the TEM are in agreement it can be concluded that the titanium particles are orienting the same way on the mica as they do on the TEM grid. This allows use of the unit cell dimensions of anatase to determine how many units thick the nanosheets are. Due to the fact that the particles have the (101) face oriented upward and that anatase has a tetrahedral unit cell it can be concluded that the (101) planes would run perpendicular to the imaged face and along the horizontal axis of the nanosheets. Using the lattice parameters for anatase the corresponding d-spacing was calculated to be 0.351 nm. By dividing the mean height of the nanosheets as measured by AFM it was possible to estimate the height of the nanosheets in unit cells. The AFM measurements for the colloid indicate that the sheets are on average 4 unit cells tall with some measuring as small as 1 unit cell and others as tall as 9 unit cells. The precipitated sheets were found to be slightly thicker with an average thickness of 11 unit cells, a minimum of 4 unit cells and a maximum of 16 unit cells. These measurements combined with the TEM data indicate that aging the titanyl sulfate solution at 60 °C produced anatase nanosheets. These sheets are severely truncated in one crystallographic direction and this might lead to interesting and unique properties.

Raman spectroscopy is very sensitive to the crystallinity and microstructure of a sample. Due to the fact that Raman peaks become very broad and shrink in intensity when local imperfections exist Raman spectroscopy can be used as a good indicator for crystallinity in samples of anatase. The Raman spectrum of the precipitated material (Figure 5) had characteristic peaks for crystalline anatase at 157, 399, 519, and 639 cm^{-1} and matched that reported by Zhang et al. The three higher frequency peaks are well resolved indicating the nanocrystals have good crystallinity with few defects[22-23]. The broadening that is observed in the spectrum and the shift in the $Eg_{(1)}$ peak at 157 cm^{-1} from 151 cm^{-1} in the precipitated anatase is an indication of nanocrystalline anatase. By comparing the peak shift from our results to that of literature values gathered by Swamy et al. shifts for nanocrystalline anatase in the E_{g1} peak to 157 cm^{-1} is indicative of samples that are around 5 nm in diameter. The full width at half maximum measurement of this peak was found to be 32 cm^{-1} and is also consistent with a particle diameter of 5 nm. This is in agreement with the XRD and AFM measurements and supports the presence of anatase.

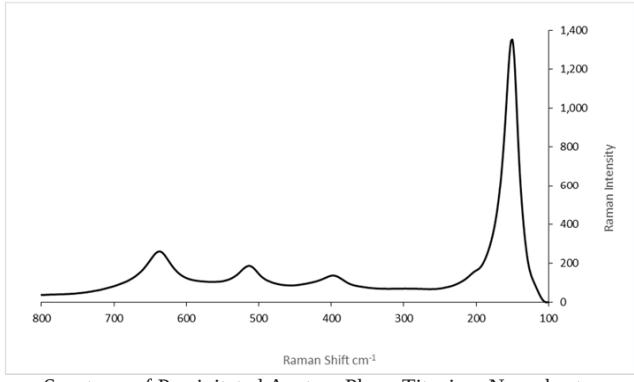

Figure 5: Raman Spectrum of Precipitated Anatase Phase Titanium Nanosheets

The infrared spectrum of the titanium dioxide precipitate was measured (Figure 5.7) and was

compared to literature values.[24-25] The spectrum has a broad peak from 3100-3500 cm^{-1} that corresponds to O-H stretching of either free or bound hydroxyl groups. This is also shown by the small peak at 1630 cm^{-1} that is due to the bending vibration of coordinated water and Ti-OH groups. The wide peak from 735 to 400 cm^{-1} can be assigned to Ti-O vibrations. From the FT-IR results we can determine that the as prepared titanium has the characteristic peaks for titanium dioxide and that there is water present in the sample in either a bound or unbound state.

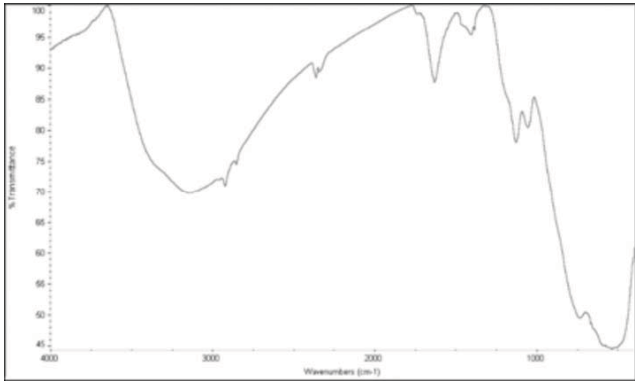

Figure 6. FT-IR Spectrum of Precipitated Titanium Nanosheets in a KBr pellet

Surface area measurements of the precipitate were performed using nitrogen BET. A six point BET measurement gave a surface area of 124 m^2/g. Degussa P-25 was used as a reference and was found to have a surface area of 55 m^2/g.

Dynamic light scattering measurements of both the suspended aggregates and the colloid were in agreement wit the previously discussed results for the size of particles from TEM and AFM measurements. The particle size distribution (Figure 7) of the precipitated titanium aggregates as a suspension in deionized water was determined using a Malvern HPP5001 dynamic light scattering instrument. The particles were found to range in size from 200 to 350 nm. The colloid nanoparticles were run as is and were found to have a distribution of particles in the range of 6.5 to 11.7 nm (Figure 7).

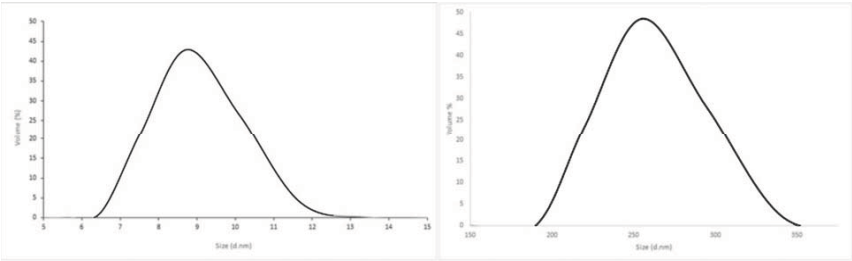

Figure 7. Dynamic Light Scattering Measurements of the Colloid Titanium Nanosheets (Left) and the Precipitated Titanium Nanosheets (Right)

The UV-Visible spectrum of the colloid and the suspended nanoparticles was recorded and the data was used to plot $(\alpha E_{phot})^2$ versus E_{phot}, which is the method typically used to determine the band gap of direct band gap semiconductors. In the calculations E_{phot} is equal to $(1293/\lambda)$ where λ is the wavelength in nanometers and α is equal to the absorption coificient. To determine the band gap, the linear portion of the curve called the adsorption edge is extrapolated to the x-intercept to determine the band gap of the titanium samples (Figure 8). Anatase is known to undergo an indirect band gap transition in bulk phase but nanometric anatase behaves as an direct band gap semiconductor according to Reddy[26]. This transition from indirect to direct band gap transition is attributed to quantum confinement that occurs in nanometric particles and is also observed in silicon nanocrystals as well[27]. Bandgaps are obtained by extrapolating the linear portion of the adsorption edge to the x-intercept. The band gap for the synthesized colloid was determined to be 3.82 eV and 3.49 eV for the aggregates. This is shifted as expected from the literature values of 3.2 eV for bulk anatase. The large shift in the band gap up to 3.82 eV for the colloid is higher than normal for titanium dioxide nanoparticles but matches literature values for nanosheets[28]. This higher than normal shift can be attributed to the 2D quantum confinement resulting from the thinness of the nanosheets. Sakai reported that the band gap for this material with less than 10 unit cell layers are approximately 3.82eV[28]. This data fits with the sizes measure for the colloid nanosheets that are on average 4 units cells in height with a maximum height of 11 unit cells. This data is particularly interesting in the case of the larger nanosheets from the precipitated nanosheets. The precipitated nanosheets have crystallite diameters of 35 nm or more, band gap shifts for anatase particles in this size range are typically reflective of the bulk particles with a band gap close to 3.2 eV[29]. The much higher band gap of 3.49 eV is not observed for particles in this size range but is due to 2D quantum confinement resulting from the nanosheets structure the particles have a much higher band gap than expected.

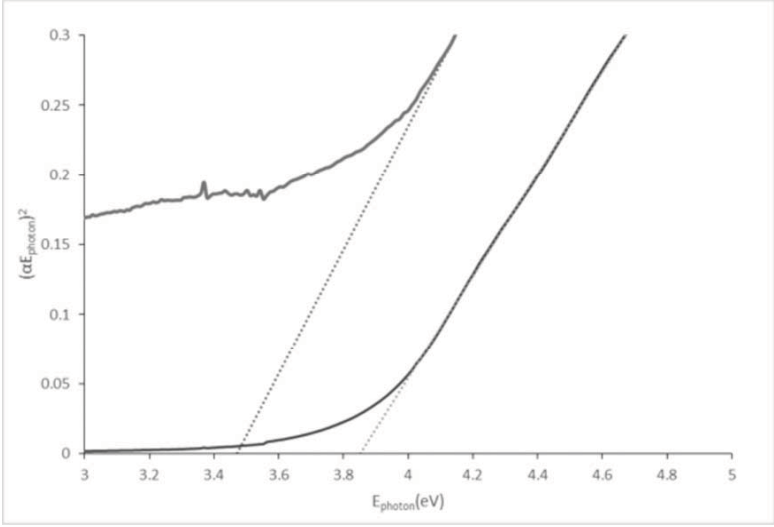

Figure 8. Plot of $(\alpha Ephot)^2$ versus Ephot for a direct band gap transition. Colloid Titanium Nanosheets (Lower Curve) and the Precipitated Titanium Nanosheets (Higher Curve)

CONCLUSION

Anatase nanosheets were successfully synthesized via isothermal aging of a titanyl sulfate solution at 60 °C. The process produced two distinct titanium products a stable colloid composed of anatase nanosheets that were on average 1.53 nm or approximately 4 unit cells in height. Due to a preferential growth axis the nanosheets imaged by TEM displayed the (101) face of anatase. The colloids had a markedly high band gap of 3.82 eV which is higher than typical for nanoparticles of similar dimensions and was only reported in one other synthesis for nanosheets. This increase in the band gap can be contributed to the 2D quantum confinement of the nanosheets.

The precipitated solid was also characterized and determined to be anatase nanosheets. The nanosheets in the precipitates were found to be on average 3.93 nm in thickness. This equates to roughly 11 unit cells on average. The precipitates tended to form aggregates that were on average 96.9 nm in diameter as measured by AFM. The sheets in both cases were found to have a preferential growth axis and the lattice fringes of the (101) anatase planes were very evident in the TEM images of both materials. The aggregated anatase nanosheets were found to be photocatalytic and were able to oxidize methylene blue. Titanium nanosheets with (101) exposed faces are of particular interest for many applications including dielectrics, photovoltaics, and photocatalysis due to the many exposed defects on the surface giving rise to unique properties.

REFERENCES

[1]A. Fujishima, and K. Honda, Electrochemical Photolysis of Water at a Semiconductor Electrode, *Nature*, ***238***, 37-+ (1972).

[2]V. J. Nagpal, R. M. Davis, and S. B. Desu, Novel Thin Films of Titanium Dioxide Particles Synthesized by a Sol-Gel Process, *Journal of Materials Research*, ***10***, 3068-3078 (1995).

[3]J. Xiao, W. Chen, F. Wang, and J. Du, Polymer/Tio2 Hybrid Nanoparticles with Highly Effective Uv-Screening but Eliminated Photocatalytic Activity, *Macromolecules*, ***46***, 375-383 (2013).

[4]R. Andreozzi, V. Caprio, A. Insola, and R. Marotta, Advanced Oxidation Processes (Aop) for Water Purification and Recovery, *Catalysis Today*, ***53***, 51-59 (1999).

[5]V. B. Gaikwad, and G. H. Jain, in *Sensing Technology (ICST), 2011 Fifth International Conference on*, **2011**, pp. 239-244.

[6]B. O'Regan, and M. Gratzel, A Low-Cost, High-Efficiency Solar Cell Based on Dye-Sensitized Colloidal Tio2 Films, *Nature*, ***353***, 737-740 (1991).

[7]S.-H. A. Lee, N. M. Abrams, P. G. Hoertz, G. D. Barber, L. I. Halaoui, and T. E. Mallouk, Coupling of Titania Inverse Opals to Nanocrystalline Titania Layers in Dye-Sensitized Solar Cells†, *The Journal of Physical Chemistry B*, ***112***, 14415-14421 (2008).

[8]T. P. Chou, Q. Zhang, B. Russo, G. E. Fryxell, and G. Cao, Titania Particle Size Effect on the Overall Performance of Dye-Sensitized Solar Cells, *The Journal of Physical Chemistry C*, ***111***, 6296-6302 (2007).

[9]A. P. Alivisatos, Semiconductor Clusters, Nanocrystals, and Quantum Dots, *Science*, ***271***, 933-937 (1996).

[10]A. P. Alivisatos, Perspectives on the Physical Chemistry of Semiconductor Nanocrystals, *J Phys Chem-Us*, ***100***, 13226-13239 (1996).

[11]Y. Yin, and A. P. Alivisatos, Colloidal Nanocrystal Synthesis and the Organic-Inorganic Interface, *Nature*, ***437***, 664-670 (2005).

[12]J. Ovenstone, and K. Yanagisawa, Effect of Hydrothermal Treatment of Amorphous Titania on the Phase Change from Anatase to Rutile During Calcination, *Chemistry of Materials*, ***11***, 2770-2774 (1999).